The antiproliferative activity of Varronia dardani (Taroda) J.S. Mill. roots against human melanoma cells and the isolation of a new hydroanthraquinone

Carlos Arthur Gouveia Veloso, César Augusto Gonçalves Dantas, Raimundo Gonçalves de Oliveira Júnior, Vicente Carlos de Oliveira Costa, Luiz Antonio Miranda de Souza Duarte-Filho, José Iranildo Miranda de Melo, Pierre Edouard Bodet, Josean Fechine Tavares, Marcelo Sobral da Silva, Laurent Picot

The antiproliferative activity of *Varronia dardani* (Taroda) J.S. Mill. roots against human melanoma cells and the isolation of a new hydroanthraquinone

Carlos Arthur G. Veloso [1,2], César Augusto G. Dantas [1], Raimundo G. de O. Júnior [3], Vicente Carlos de O. Costa [1], Luiz A. M. S. Duarte-Filho [2], José Iranildo M. de Melo [4], Pierre E. Bodet [5], Josean F. Tavares [1], Marcelo S. da Silva [1], Laurent Picot [2*]

[1] PPgPNSB, Universidade Federal da Paraíba, 58000-000 João Pessoa, Paraíba, Brazil;

[2] La Rochelle Université, UMR CNRS 7266 LIENSs, 17042 La Rochelle, France;

[3] UMR CNRS 8038 CITCOM, Université Paris Cité, 75006 Paris, France;

[4] CCBS, Universidade Estadual da Paraíba, 58429-500 Campina Grande, PB, Brazil;

[5] Plateforme d'analyse haute résolution des biomolécules, La Rochelle Université, UMR CNRS 7266 LIENSs, 17042 La Rochelle, France.

Correspondance: [*] laurent.picot@univ-lr.fr

Abstract: The Caatinga is a unique Brazilian semi-arid biome in the north-east of the country, containing endemic plant species. Among these, Cordiaceae are traditionally used by local communities for the treatment of various diseases such as gastric pain, menstrual colic and arthritis. In this work, the antiproliferative activity of the species *Varronia dardani* was evaluated in chemoresistant human melanoma cells. The ethanolic extract of *V.dardani* root exerted high antiproliferative activity in A2058 cells and was selected for further phytochemical characterization and bioguided purification of antimelanoma compounds. The isopropanol fraction was the most active and contained a novel hydroanthraquinone which was isolated, characterized and named vardanone. This molecule is the first hydroanthraquinone reported in *V. dardani* and UPLC-MS/MS analysis revealed that it was composed of a mixture of isomers. When tested in melanoma cells, vardanone didn't induce the inhibition of A2058 cell growth, indicating that the fraction's antimelanoma activity is attributable to other molecules which will be further characterized. This study is the first to demonstrate the presence of a hydroanthraquinone in *V. dardani* and paves the way for the identification of new antimelanoma phytochemicals in this species.

Keywords: Cordiaceae, natural products, hydroanthraquinone, melanoma, *Varronia*.

1. Introduction

Despite the development of effective anti-cancer drugs and the significant progress made over the past 25 years in the prevention, diagnosis and clinical management of cancer, chemoresistant tumors still represent the second leading cause of death in developed countries. The number of cases is expected to increase significantly in the near future, driving the ongoing search for new effective drugs. Cutaneous melanoma is a good example of aggressive tumor that represents a major public health problem (Clark et al., 1975; Locatelli et al., 2013). In Europe, over 20,000 people die from melanoma every year (Grange, 2005) and it is the most common tumor in young adults aged 25 to 35, responsible for 80% of skin cancer mortality (Grange, 2005; Locatelli et al., 2013). The incidence of melanoma is increasing worldwide, and the only effective treatment is early surgical resection of primary melanoma, when tumor cells have not spread to lymph nodes (stages I and II) (Clark et al., 1975; Knight et al., 2015). Indeed, metastatic melanoma (stages III and IV) has a very poor prognosis as most chemotherapeutic agents are ineffective at killing melanoma cells, which are constitutively drug-resistant or rapidly develop chemoresistance (Balch et al., 2009, 2001; Clark et al., 1975; Manola et al., 2000). Although the recent development of targeted drugs (c-Kit, B-raf and MEK inhibitors) has increased life expectancy of patients (Davies et al., 2002; Haluska et al., 2006; Mckee et al., 2013; Menzies and Long, 2013), the efficacy of these treatments is short-lived due to the acquisition of resistance after a few months (Palmieri et al., 2015). Promising results for the treatment of melanoma are also arising from immunotherapy strategies and the combination of immunotherapy with chemotherapy (Knight et al., 2015; Menzies and Long, 2013; Nardin et al., 2011; Prickett et al., 2016), confirming the interest in identifying new natural products with cytotoxic, cytostatic, antimetastatic or antiangiogenic activities that could be used synergistically with immunotherapy (Alqathama and Prieto, 2015).

In this view, medicinal plants represent a major resource for the identification of anti-cancer molecules and the development of innovative drugs. With regard to melanoma, various classes of natural secondary metabolites found in medicinal plants have been described as potent cell cycle blockers and inhibitors of biochemical pathways involved in cell proliferation, survival and chemoresistance (Alqathama and Prieto, 2015; de Oliveira Júnior et al., 2019; de Oliveira-Júnior et al., 2022; Júnior et al., 2017; Van Goietsenoven et al., 2010). Brazil, with about 20% of known living species, is a hotspot for biodiversity and a major source of original plants containing bioactive substances (Bolzani et al., 2012; Valli et al., 2013). Among Brazilian plants of medicinal interest, the Cordiaceae family includes trees or shrubs with a tropical distribution that are present in all Brazilian states (Watanabe et al., 2017). This family was traditionally considered a subfamily of the Boraginaceae, but recent molecular studies have elevated it to the family status (De Melo et

al., 2018). In northeastern Brazil, many Cordiaceae are commonly used in folk medicine to treat gastrointestinal, urogenital, respiratory, cardiac and vascular diseases and their extracts were shown to exert antimicrobial, anti-inflammatory, anthelmintic, diuretic and analgesic properties. Various classes of secondary metabolites have been isolated and characterized from different parts of plants in this family, including lignans, naphthoquinones, chromones, saponins, terpenoids, alkaloids, flavonoids and phenolic compounds (Do Vale et al., 2012; Matias et al., 2015). In this family, the genus *Varronia* comprises around 125 neotropical species (Miller and Gottschling, 2007), 30 of which occur in Brazilian biomes, more than half of which are endemic and distributed in four main phytogeographic domains (Amazonian forest, atlantic forest, cerrado and caatinga). Six species are endemic to northeastern Brazil, including *Varronia dardani* and *V. leucocephala* (De Oliveira Chagas and Da Costa-Lima, 2018; Vieira et al., 2015). *Varronia* are particularly used in folk medicine as antiulcer, antimicrobial, antifungal, larvicidal, anti-inflammatory and analgesic (Freitas et al., 2012); however, only few studies have highlighted their anticancer potential and only Cordiaquinone J, isolated from *V. leucocephala*, has been shown to induce apoptosis and necrosis in leukemia cells through the production of reactive oxygen species (Marinho-Filho et al., 2010).

Therefore, in the present work, *Varronia dardani* was selected to evaluate its potential antiproliferative activity in a model of human chemoresistant melanoma cell line. We discovered that *V. dardani* root ethanolic extract and its isopropanolic fraction induce a high growth inhibition of A2058 human metastatic melanoma cells at 100 µg.mL^{-1}. Following a fractionation strategy, a novel hydroanthraquinone we named vardanone was isolated and characterized from the isopropanolic fraction. However, purified vardanone showed no significant inhibition of A2058 cell growth, indicating that the fraction's antimelanoma activity was attributable to other molecules which are currently characterized. This study is the first to report the presence of a hydroanthraquinone in *V. dardani* and paves the way for the identification of original antimelanoma phytochemicals in this species.

2. Materials and Methods

2.1 Plant material

The roots of *Varronia dardani* (Taroda) J.S. Mill., Cordiaceae, were collected in the municipality of Serra Branca, Paraíba, Brazil (latitude 7°29'14" S and longitude 36°39'51" W) in March 2016. A specimen was analyzed, identified by the botanist Prof. Dr. José Iranildo Miranda de Melo and stored at the Herbarium Prof. Lauro Pires Xavier (JPB) of Federal University of Paraíba (UFPB) under the number JPB 29509. The access to the botanical material was authorized

by Sistema Nacional de Gestão do Patrimônio Genético e do Conhecimento Tradicional Associado (SISGEN) and was registered under number A0E7358, as required for Brazilian legislation.

2.2 Extraction and fractionation

The roots (410 g) were dehydrated in an oven with circulating air at a temperature of 40 ºC for 72 hours and pulverized. The dried material was macerated with ethanol for 72 hours and the extractive solution was concentrated, resulting in 57.8 g of ethanolic extract (EE), with a yield of 14.1%. The extract was subjected to flash chromatography fractionation using an Interchim Puriflash® PF430 system and a silica column (12 g, 15 µm) equipped with an automatic collector (10 mL per tube) to obtain one isopropanol fraction (EE-I); one isopropanol:methanol fraction (EE-IM); one methanol fraction (EE-M) and one aqueous fraction (F-A). The elution was monitored at 350 nm, using a fixed flow rate (10 $mL.min^{-1}$) with a mobile phase composed of a ternary solvent gradient: A (isopropanol), B (methanol) and C (water) and the following gradient program: 0 – 30 min, 100% A; 30–35 min, 100% A to 50%A : 50% B, 35 – 65 min 50% A : 50% B, 65-70 min 50% A : 50% B to 100% B; 70 – 100 min, 100% B; 100 – 105 min, 100% B to 100% C; 105 – 135 min, 100% C. Fractions were dried using a rotary evaporator before dilution in the cell culture medium for the biological evaluation.

A 560 mg aliquot of the isopropanol fraction from the ethanolic extract of *V. dardani* roots (EE-I), considered the most active in the MTT test, was subjected to fractionation using the methodology described previously and mobile phase composed of a gradient of solvents: A (cyclohexane) and B (ethyl acetate), using the following gradient program: 0 – 10 min, 5% B; 10–15 min, 5% to 10% B; 15 – 25 min 10% B; 25-30 min, 10% to 35% B; 30 – 40 min, 35% B; 40 – 45 min, 35% to 65% B; 45 – 55 min, 65% B; 55 – 60 min, 65% to 90% B; 60 – 70 min, 90% B; 70 – 75 min, 90% to 100% B; 75 – 80 min, 100% B. Seventy-nine tubes were collected, each containing 10 mL. The fractions were dried using a rotary evaporator at 45 ºC and then pooled into 11 subfractions (EE-I-Fr.01 to EE-I-Fr.11) according to the chromatographic profiles analyzed by thin layer chromatography (TLC) with silica gel in aluminum support plates (Merck® with F-254 indicator, 200 µm thickness and 20x20 cm in size). After elution, the plates were revealed by exposure to UV light at wavelengths 254 and 366 nm in the BOIT-LUB01 device from Boitton. The fraction EE-I-Fr.02 had the best chromatographic profile and was chosen to be submitted to a preparative TLC using preparative plates of silica gel 60 with indicator F-254 (Merck®) and a binary mixture of cyclohexane:ethyl acetate (9:1). After elution, the plates were revealed by exposure to UV light at wavelengths 254 and 366 nm. Four spots (EE-I-Fr.02-M1 to EE-I-Fr.02-M4) were collected and analyzed by ^{1}H and ^{13}C NMR. This analysis demonstrated that only the

spot EE-I-Fr.02-M3 was a purified molecule, the other spots containing mixtures. EE-I-Fr.02-M3 was thus selected for further structural characterization.

2.3 Structural analysis

The ^{1}H and ^{13}C NMR spectra of the isolated compound were recorded on a Bruker Ascend 400 spectrometer at 400 MHz and 100 MHz, respectively, in $CDCl_3$, using tetramethylsilane (TMS) as the internal standard. The infrared analyses were obtained in the region (4000 to 400 cm^{-1}) using an IRPrestige-21 equipment (Shimadzu), using 1 mg of sample on KBr pellets, with the frequency measured in cm^{-1}. MS data were recorded on a Bruker high-resolution mass spectrometer, micrOTOF II model using the Electrospray Ionization technique. The micrOTOF II analysis parameters were: capillary 4.0 kV, IES in negative mode, end plate offset 500 V, nebulizer 35 psi, dry gas (N_2) with a flow rate of 8 $L.h^{-1}$ and temperature of 300 °C. Spectra (m/z 50-1000) were recorded every 2 seconds.

2.4 UPLC-MS/MS analysis of vardanone

EE-I-Fr.02-M3 was analyzed using an Acquity UPLC HClass (Waters, Milford, USA) coupled to a Waters 2996 photodiode array detector or a Xevo G2 S Q-TOF mass spectrometer, equipped with an electrospray ionization (ESI) source (Waters, Manchester, England). The chromatographic system consisted of a quaternary pump (Quaternary Solvent Manager, Waters) and an automatic injector (Sample Manager-FTN, Waters) equipped with a 10 μL sample loop. The sample was dissolved in acetonitrile:water (5:95; v/v) to obtain a 100 μM solution and 5 and 10 μL (for MS and UV analysis, respectively) were injected in a C18 column (Acquity UPLC BEH C18, Waters) (2.1 × 50 mm, 1.7 μm), using a flow rate of 0.3 $mL.min^{-1}$. The elution gradient was composed of solvents A (0.001% formic acid in water) and B (0.001% formic acid in acetonitrile) as follows: 0–3 min, 5% B; 3–7 min, 5–10% B; 7–10 min, 10% B; 10–12 min, 10-15% B; 12–14 min, 15% B; 14–16 min, 15–20% B; 16–19 min, 20% B; 19–21 min, 20–30% B; 21–23 min, 30% B; 23–26 min, 30–90% B; 26–29 min, 90% B; 29–30 min, 90–5% B; 30–35 min, 5% B. The column was kept at 25 °C, during all analyses. UV spectra acquisition was performed in a 220–800 nm interval (10 spectra/s). All MS analyses were performed in the positive and negative ionization mode. Final ESI conditions were: source temperature 120 °C, desolvation temperature 500 °C, cone gas flow-rate 50 $L.h^{-1}$, desolvation gas flow-rate 300 $L.h^{-1}$, capillary voltage 3 kV (positive mode) end 2.5 kV (negative mode), sampling cone voltage 35 V, and source compensation 80 V. The instrument was set to acquire over the m/z 50–1200 range with a scan time equal to 0.1 s. Ramp collision energy was from 10 to 40 V.

2.5 Antiproliferative assay

The antiproliferative activity of extracts and fractions was studied using the A2058 cell line (ATCC® CRL-11147). A2058 are highly invasive human epithelial adherent melanoma cells, derived from lymph nodes metastatic cells obtained from a 43 years male patient. They are tumorigenic at 100% frequency in nude mice, considered as very resistant to anticancer drugs and contain the V600E BRAF mutation. All cell culture experiments were performed at 37°C. Cells were grown to confluence in 75 cm² flasks in DMEM medium supplemented with 10% fetal bovine serum (FBS) and 1% antibiotic solution (penicillin-streptomycin) (Dominique Dutscher, France), in a humidified atmosphere with 5% CO_2. The extracts were solubilized in DMSO at 10 $mg.mL^{-1}$ and diluted in the cell culture medium to obtain solutions with 200 $\mu g.mL^{-1}$. Confluent cells were trypsinized and centrifuged 1,500 g for 5 minutes. The supernatant containing trypsin was discarded and the cell pellet was resuspended in cell culture medium to obtain a suspension at $4,10^4$ $cells.mL^{-1}$. At T_0, 50 µL of the extract solutions at 200 $\mu g.mL^{-1}$ were deposited into a 96-well flat-bottom microplate to obtain a final concentration of 100 $\mu g.mL^{-1}$ and 50 µL of the cell suspension was added. The added 2000 cells were then cultured for 72 h in the cell culture medium containing the extracts. After 72 h, 20 µL of a 5 $g.L^{-1}$ MTT solution was added to each well of the microplate for 4 h. The cell culture medium was then removed and the formazan crystals were dissolved in 200 µL of DMSO. The microplates were incubated at 37 °C for 5 minutes to solubilize the formazan crystals and the absorbance was read at 550 nm using a FLUOstar Omega microplate reader (BMG Labtech®, France). Photomicrographs after the treatments were taken on a Nikon Eclipse TS100 inverted microscope (x100 magnification) equipped with a digital camera. Purified vardanone was solubilized at 10^{-3} M in DMSO and tested in melanoma cells at final concentrations of 10 and 20 µM. Data were expressed as % growth inhibition as compared to control untreated cell from the mean ± SEM from three independent experiments.

3. Results and Discussion

3.1 Antiproliferative assay with the extract and fractions

The overall strategy was to evaluate the antiproliferative activity in A2058 melanoma cells of the ethanolic extract and fractions from *Varronia dardani* roots. The morphological changes of melanoma cells treated with the extract and fractions were also evaluated by microscopic observations and compared with untreated control cells. The ethanolic extract of *V. dardani* roots (EE) induced 86.13 ± 5.37% growth inhibition in chemoresistant melanoma cells. Its isopropanolic fraction (EE-I) and isopropanol:methanol fraction (EE-IM) also exerted a high antiproliferative

activity at 72 h with 78.18 ± 3.17 and 70.94 ± 3.91% of growth inhibition, respectively. In contrast, the most polar fractions (EE-M and EE-A) exerted a very low antiproliferative activity (**Table 1**).

Table 1. Growth inhibition of A2058 cells treated for 72 h with *Varronia dardani* roots ethanolic extract and fractions at 100 µg.mL^{-1}.

Sample	Growth inhibition at 100 µg.mL^{-1} after 72 h of treatment (% control ± SEM, n=3)
EE	86.13 ± 5.37
EE-I	78.18 ± 3.17
EE-IM	70.94 ± 3.91
EE-M	0.88 ± 4.08
EE-A	4.79 ± 3.32

EE: Ethanolic extract of *V. dardani* roots; EE-I = Isopropanolic fraction of *V. dardani* ethanolic extract; EE-IM: Isopropanol:methanol fraction of *V. dardani* ethanolic extract; EE-M: methanolic fraction of *V. dardani* ethanolic extract; VD-R-A: aqueous fraction of *V. dardani* extract.

The ethanolic extract of *V. dardani* roots (EE) and its isopropanolic fraction (EE-I) (1-100 µg.mL^{-1}) reduced the number of viable A2058 cells in a concentration-dependent manner when compared to the control group, exhibiting a IC_{50} of 19.92 µg.mL^{-1} and 18.72 µg.mL^{-1}, respectively (**Fig. 1**).

Fig. 1. Growth inhibition of A2058 cells after exposure to increasing concentrations (1-200 µg/mL, 72 h) of the ethanolic extract of *V. dardani* roots (EE) and its isopropanolic fraction (EE-I). Results are expressed as mean ± SEM, tests were performed in triplicate (n = 3).

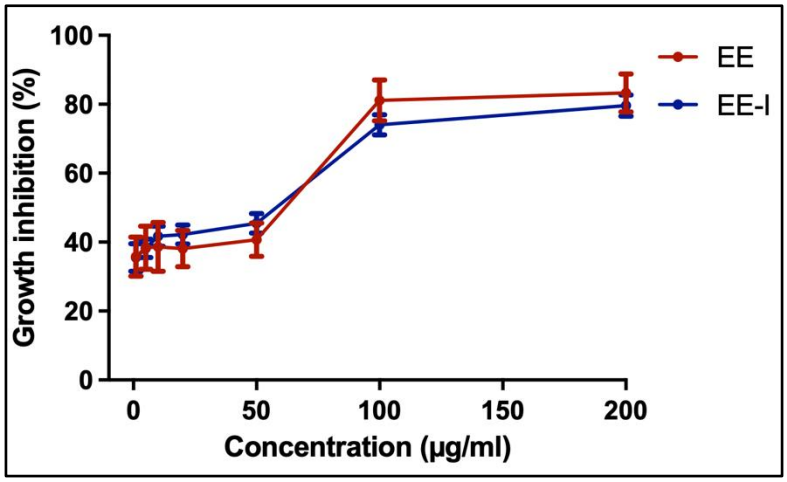

After observation of the treated cells, it was possible to confirm the cytotoxicity of the ethanolic extract (EE) and its isopropanolic fraction (EE-I), due to the fact that untreated cells exhibited regular epithelial morphology and became sub-confluent after 72 h, indicating a high proliferation rate, and in contrast, treatments with EE and EE-I (50 and 100 μg.mL^{-1}) caused a reduction in cell density, cell shrinkage and rounding (**Fig. 2**). Considering the high antiproliferative activity demonstrated by the ethanolic extract and its more apolar fraction (EE-I), the latter sample was selected for isolation of compounds with possible antimelanoma activity.

Fig. 2. Treatments with ethanolic extract of *V. dardani* roots (EE) and its isopropanolic fraction (EE-I) caused reduction in cell density, cell shrinkage and rounding (black arrows).

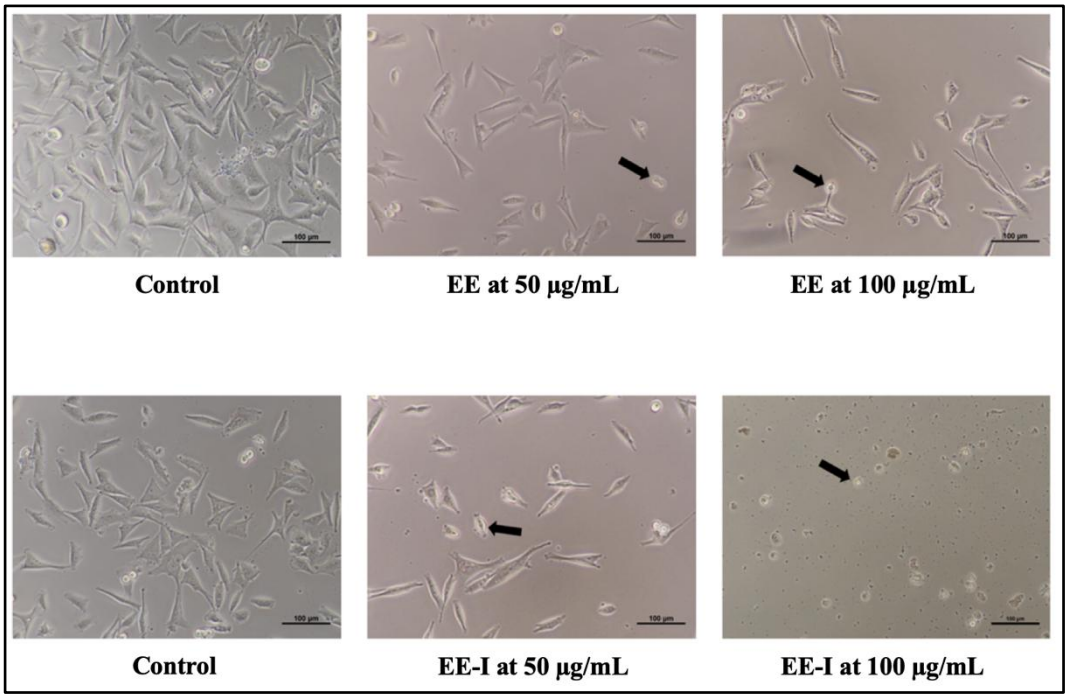

3.2 Structural analysis

Following the fractionation and TLC analysis of EE-I, the EE-I-Fr.02-M3 purified molecule was obtained as a yellow powder (16 mg, yield 0,0277%), and its HRMS displayed a molecular ion peak at m/z $[M+H]^+$ compatible with the molecular formula $C_{17}H_{21}O_5$ (calcd. 305.1384, error = -0,1 ppm) (**Fig. 3**).

Fig. 3. IES-MS spectra of EE-I-Fr.02-M3 (vardanone).

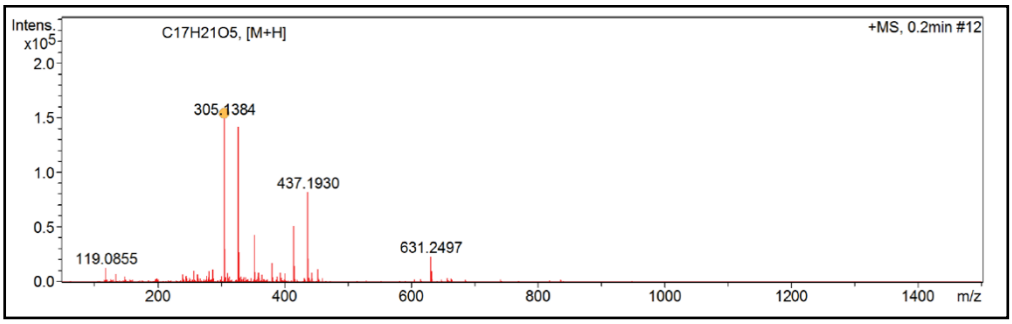

In the ^{1}H NMR spectrum (400 MHz, $CDCl_3$) two unshielded signals could be observed, δ_H 12.38 and δ_H 11.49, each integrating to one hydrogen, already known as chelated hydrogens with carbonyls of a basic core of anthraquinones and naphthoquinones (Borgati et al., 2019; Procházková et al., 2021). Also, in the ^{1}H NMR spectrum only one signal was observed in the aromatic proton region, integrating to a hydrogen, at δ_H 6.62 (s). The spectroscopic data also revealed the presence of a 1,2,3,4,6-pentisubstituted aromatic ring. A simplet at δ_H 3.93, integrating to three hydrogens, was observed, which was related to the presence of a methoxyl group. Therefore, from the ^{1}H NMR spectrum, it was possible to suggest that the skeleton of the EE-I-Fr.02-M3 resembled that of a methoxylated anthraquinone (Ji et al., 2022).

The ^{13}C APT NMR spectra (100 MHz, CD_3OD) of EE-I-Fr.02-M3 showed 17 signals that were assigned to 17 carbons, as follows: 8 signals for non-hydrogenated carbons (-C), 3 signals for methynic carbons (-CH), 3 signals for methylenic carbons ($-CH_2$), 2 signals for methyl carbons ($-CH_3$), and 1 signal for methoxy carbon ($-OCH_3$). The three characteristic methylenic carbon shifts, δ_C 34.80, δ_C 20.14, and δ_C 32.42, were assigned to the C-2, C-3, and C-4 carbons, respectively, of the A ring, which indicated its absence of unsaturation. The other carbons of the same ring were suggested through the signals at δ_C 27.07, δ_C 48.16 and δ_C 59.22, which were assigned to carbons C-1, C-4a and C-9a. In the same spectrum, non-hydrogenated aromatic carbon signals were observed at δ_C 115.19, δ_C 144.07, δ_C 156.42, δ_C 158.08 and δ_C 105.22, which were assigned respectively to carbons C-5a, C-5, C-6, C-8 and C-8a of the C ring. The C-7 carbon of the same ring was suggested by the signal at δ_C 106.00. Also, in the ^{13}C NMR spectrum, two characteristic carbonyl carbon signals were observed, one at δ_C 206.27 and the other at δ_C 204.40, assigned to carbons C-9 and C-10, respectively (Borgati et al., 2019; Ji et al., 2022; Procházková et al., 2021). All the ^{1}H and ^{13}C NMR data are shown in **Table 2**.

In the contour map of the HMBC spectra, it was possible to observe the correlation between the signals of the hydrogens at δ_H 3.93 with the carbon signal δ_C 156.42, indicating that the methoxyl group would be inserted in the C-6 carbon on the C ring (Li et al., 2019). Also, in the

same contour map, correlations were observed, which indicated the insertion of a methyl at carbons C-1 (δ_H 1.17 and δ_C 21.64) and C-4a (δ_H 1.16 and δ_C 19.78). The positions of the chelated hydroxyls were established by correlating the signals at δ_H 11.49 (5-OH) and δ_C 204.40 (C-10); and δ_H 12.38 (8-OH) and δ_C 206.27 (C-9) (Ji et al., 2022; Wisetsai et al., 2021). All these correlations, for better interpretation, are shown in **Fig. 4** by curved arrows. All these correlations were also confirmed by the HSQC contour map, which can be found in the Supplementary Material.

Table 2. ^{1}H, ^{13}C NMR data (400 and 100 MHz, $CDCl_3$) of EE-I-Fr.02-M3 (5,8-dihydroxy-6-methoxy-1,4a-dimethyl-1,2,3,4,4a,9,9a,10-octahydroanthracene-9,10-dione), named vardanone.

Position	δ_H	δ_C	Position	δ_H	δ_C
1	2.05 (1H, m)	27.07	**8a**	-	105.22
2	1.67 (1H, m)	34.80	**9a**	2.59 (1H, d, *J* = 10.8 Hz)	59.22
3	1.48 (1H, m)	20.14	**9**	-	206.27
	0.95 (1H, m)				
4	2.05 (1H, m)	32.42	**10**	-	204.40
	1.80 (1H, dd, *J* = 3.6 and 14 Hz)				
4a	-	48.16	**11**	1.17 (3H, s)	21.64
5	-	144.07	**12**	1.16 (3H, d, *J* = 6.9 Hz)	19.78
5a	-	115.19	**6-OMe**	3.93 (3H, s)	56.50
6	-	156.42	**5-OH**	11.49 (1H, s)	-
7	6.62 (1H, s)	106.00	**8-OH**	12.38 (1H, s)	-
8	-	158.08			

Fig. 4. Main correlations evidenced in the HMBC contour map.

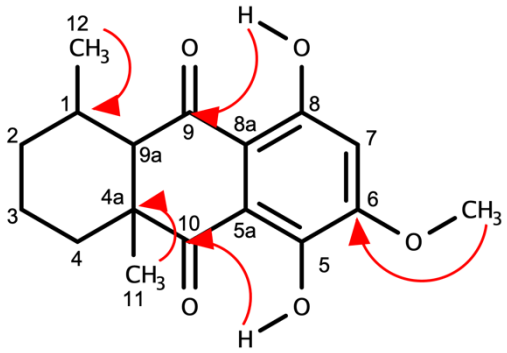

The infrared spectrum of EE-I-Fr.02-M3 showed absorption of a band at 3739 cm^{-1} characteristic of -OH group, carbonyl band at 1629 cm^{-1}, characteristic of chelated carbonyl group of quinones (Diaz-Muñoz et al., 2018), absorptions at 1463 and 1629 cm^{-1} of aromatic C=C, in addition to the signal at 1105 cm^{-1} of C-O stretching. Based on the comparison with similar structures found in the literature, the structural elucidation of EE-I-Fr.02-M3 was possible and led to the identification of a new hydroanthraquinone which we named vardanone (**Fig. 5**).

Fig. 5. Vardanone, a new anthraquinone isolated from the roots of *V. dardani*.

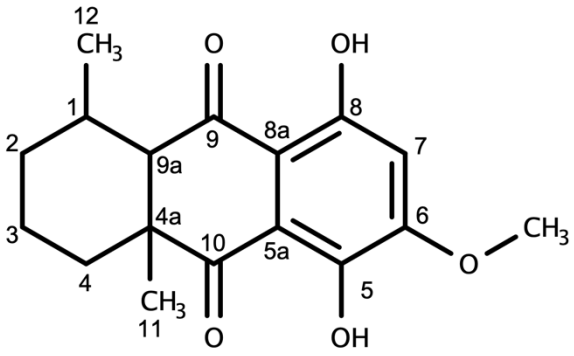

Experimental NMR and IR data of EE-I-Fr.02-M3 can be found as Supplementary Material. An attempt was made to recrystallize the molecule in order to define its absolute conformation by X-ray diffraction, but this was unsuccessful.

This is the first time that the structure of this hydroanthraquinone has been reported in the literature. The anthraquinones in plants with a single hydroxylated ring are likely originated from the shikimate or chorismate/o-succinylbenzoic acid pathways, being the latter particularly prevalent in the Rubiaceae family (Han et al., 2001). The foundational structural framework of these anthraquinones is a result of two distinct pathways, with rings A and B being produced through α-ketoglutarate and o-succinylbenzoic acid (OSB), while ring C is derived from the terpenoid pathway, utilizing isopentenyl diphosphate (IPP) (Mund and Čellárová, 2023). In the last stages of

biosynthesis, most anthraquinones undergo some changes, such as hydroxylation or methylation (Watroly et al., 2021; Zhang et al., 2022).

For centuries, this category of chemical compounds has played a pivotal role in diverse medical treatments of cancers. These compounds act by specifically targeting vital proteins within cancer cells, and scientists are actively engaged in developing new anthraquinone-based compounds with potential applications in cancer treatment (Malik et al., 2021).

3.3 UPLC-MS/MS analysis of vardanone

In the UPLC-MS/MS analysis, it was possible to determine that vardanone was actually a mixture of isomers, as indicated by the appearance of two distinct chromatographic peaks at 26.92 and 27.17 minutes (**Fig. 6**), respectively, along with their shared UV-visible absorption maximum at 393 nm.

Fig. 6. UV chromatogram of vardanone, obtained by UPLC-MS/MS (λ max = 393 nm).

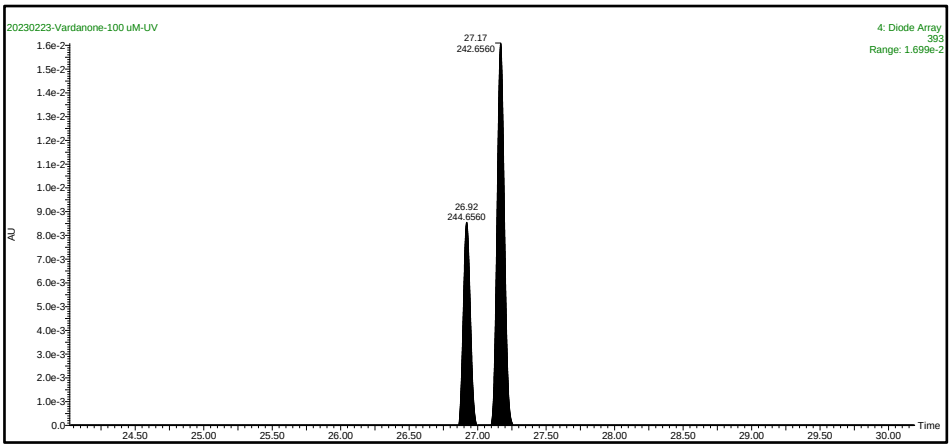

The isomerism was further supported by the mass spectrometry results, where identical molecular ion peaks at m/z 305.1385 and 303.1238 were observed in positive and negative ionization modes, respectively. MS/MS fragmentation profiles, including the relative intensities of fragment ions, also validated this hypothesis. This congruence strongly suggests a common core structure among the isomers. Therefore, further comprehensive structural elucidation techniques, such as Nuclear Magnetic Resonance (NMR) spectroscopy or computational chemistry approaches, should be undertaken to differentiate and characterize these compounds.

3.4 Antiproliferative assay with a mixture of vardanone isomers

The antiproliferative test results with a mixture of isomers of vardanone against A2058 human melanoma cells revealed a very low inhibitory effect on cell growth (**Fig. 7**).

Fig. 7. Growth inhibition of A2058 cells after exposure to mixture of vardanone isomers (10 and 20 µM, 72h).

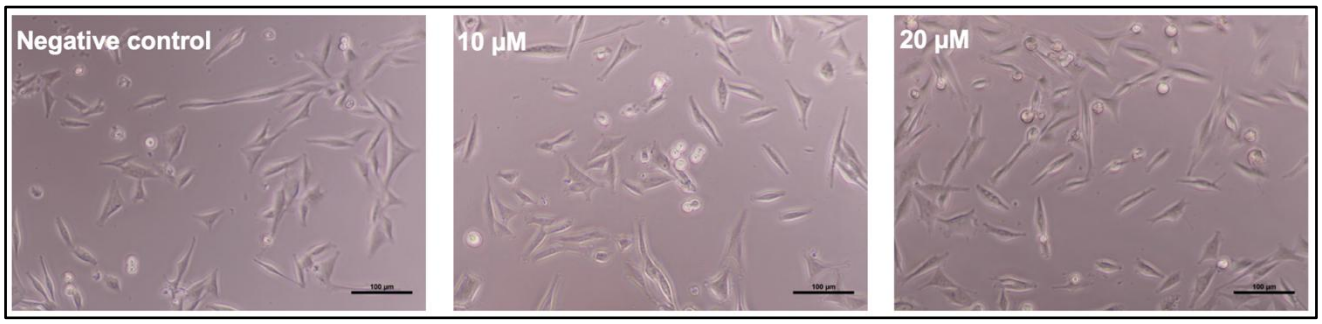

Two concentrations, 10 µM and 20 µM, were tested over a 72-hour treatment period. Both concentrations induced very low growth inhibition, with 0.92 ± 3.00% for the 10 µM and 4.39 ± 3.22% for 20 µM, indicating that this molecule doesn't interfere with cell proliferation at these concentrations (**Table 3**). Other biological activities are currently being investigated for this new molecule.

Table 3. Growth inhibition of A2058 cells after 72 h treatments with the mixture of vardanone isomers at 10 and 20 µM.

Mixture of vardanone isomers (µM)	Growth inhibition after 72 h of treatment (% control ± SEM, n=3)
10	0.92 ± 3.00
20	4.39 ± 3.22

The discrepancy between the activity of the fraction and the isolated compound vardanone on human melanoma cells clearly demonstrates that other antiproliferative molecules are present and remain to be identified in the fraction. However, this lack of antiproliferative activity doesn't mean that vardanone has no interest for cancer treatment as it could be useful for the chemosensitization of cancer cells to cytotoxic drugs (de Oliveira Júnior et al., 2019), or as a potential photosensitizer for phototherapy. These hypotheses will be further explored in our research group. Finally, for several anthraquinones isolated from medicinal plants, antioxidant activities were reported as well as potential interests for the treatment of osteoporosis or cardiovascular diseases. In this view, the discovery of vardanone opens the way for its pharmacological evaluation in various *in vitro* and *in vivo* models.

4. Conclusions

In conclusion, this study shed light on the phytochemical composition and biological activity of *Varronia dardani*, an endemic plant species found in the Caatinga biome of Brazil. The ethanolic extract of *V. dardani* roots exhibited significant antiproliferative activity against chemoresistant human melanoma cells (A2058). Further investigation led to the isolation and characterization of a novel hydroanthraquinone named vardanone from the isopropanol fraction of the ethanolic extract. Interestingly, vardanone alone did not induce the inhibition of A2058 cell growth, suggesting that the antimelanoma activity of the fraction is likely attributed to other yet-to-be-identified molecules. This discovery not only marks the first report of a hydroanthraquinone in *Varronia dardani* but also opens paths for future research to identify and characterize new phytochemicals with potential antimelanoma properties in this species. These findings not only expand the knowledge of the therapeutic potential of native flora but also emphasize the importance of conserving medicinal plants within their natural ecosystems and valorize this biodiversity for human health.

Acknowledgment

This study was financed in part by the Coordenação de Aperfeiçoamento de Pessoal de Nível Superior – Brasil (CAPES) – Finance Code 001, by the National Council for Scientific and Technological Development – Brazil (CNPq) (Process Number 200311/2022-0) and by La Ligue contre le cancer (17). The authors thank the Franco-Brazilian Network on Natural Products (FB2NP: https://fb2np.univ-lr.fr) for scientific support.

Conflict of interest

The authors declare they have no conflict of interests.

References

Alqathama, A., Prieto, J.M., 2015. Natural products with therapeutic potential in melanoma metastasis. Nat Prod Rep 32, 1170–1182. https://doi.org/10.1039/c4np00130c

Balch, C.M., Gershenwald, J.E., Soong, S.J., Thompson, J.F., Atkins, M.B., Byrd, D.R., Buzaid, A.C., Cochran, A.J., Coit, D.G., Ding, S., Eggermont, A.M., Flaherty, K.T., Gimotty, P.A., Kirkwood, J.M., McMasters, K.M., Mihm, M.C., Morton, D.L., Ross, M.I., Sober, A.J., Sondak, V.K., 2009. Final version of 2009 AJCC melanoma staging and classification. Journal of Clinical Oncology 27, 6199–6206. https://doi.org/10.1200/JCO.2009.23.4799

Balch, C.M., Soong, S.J., Gershenwald, J.E., Thompson, J.F., Reintgen, D.S., Cascinelli, N., Urist, M., McMasters, K.M., Ross, M.I., Kirkwood, J.M., Atkins, M.B., Thompson, J.A., Coit, D.G., Byrd, D., Desmond, R., Zhang, Y., Liu, P.Y., Lyman, G.H., Morabito, A., 2001. Prognostic factors analysis of 17,600 melanoma patients: Validation of the American Joint Committee on

Cancer melanoma staging system. Journal of Clinical Oncology 19, 3622–3634. https://doi.org/10.1200/JCO.2001.19.16.3622
Bolzani, V. da S., Valli, M., Pivatto, M., Viegas, C., 2012. Natural products from Brazilian biodiversity as a source of new models for medicinal chemistry. Pure and Applied Chemistry 84, 1–10. https://doi.org/10.1351/PAC-CON-12-01-11
Borgati, T.F., de Souza Filho, J.D., de Oliveira, A.B., 2019. A Complete and Unambiguous 1H and 13C NMR Signals Assignment of para-Naphthoquinones, ortho- And para-Furanonaphthoquinones. J Braz Chem Soc 30, 1138–1149. https://doi.org/10.21577/0103-5053.20190009
Clark, W.H., Ainsworth, A.M., Bernardino, E.A., Yang, C.H., Mihm, M.C., Reed, R.J., 1975. The developmental biology of primary human malignant melanomas. Semin Oncol 2, 443–450. https://doi.org/10.1016/S0046-8177(86)80032-6
Davies, H., Bignell, G.R., Cox, C., Stephens, P., Edkins, S., Clegg, S., Teague, J., Woffendin, H., Garnett, M.J., Bottomley, W., Davis, N., Dicks, E., Ewing, R., Floyd, Y., Gray, K., Hall, S., Hawes, R., Hughes, J., Kosmidou, V., Menzies, A., Mould, C., Parker, A., Stevens, C., Watt, S., Hooper, S., Jayatilake, H., Gusterson, B.A., Cooper, C., Shipley, J., Hargrave, D., Pritchard-Jones, K., Maitland, N., Chenevix-Trench, G., Riggins, G.J., Bigner, D.D., Palmieri, G., Cossu, A., Flanagan, A., Nicholson, A., Ho, J.W.C., Leung, S.Y., Yuen, S.T., Weber, B.L., Seigler, H.F., Darrow, T.L., Paterson, H., Wooster, R., Stratton, M.R., Futreal, P.A., 2002. Mutations of the BRAF gene in human cancer. Nature 417, 949–954. https://doi.org/10.1038/nature00766
De Melo, J.I.M., Paulino, R.D.C., De Oliveira, R.C., Vieira, D.D., 2018. Flora of Rio Grande do Norte, Brazil: Boraginales. Phytotaxa 357, 235–260. https://doi.org/10.11646/phytotaxa.357.4.1
De Oliveira Chagas, E.C., Da Costa-Lima, J.L., 2018. A New Species of Varronia (Cordiaceae, Boraginales) from Northeastern Brazil. Syst Bot 43, 1026–1029. https://doi.org/10.1600/036364418X697760
de Oliveira Júnior, R.G., Bonnet, A., Braconnier, E., Groult, H., Prunier, G., Beaugeard, L., Grougnet, R., da Silva Almeida, J.R.G., Ferraz, C.A.A., Picot, L., 2019. Bixin, an apocarotenoid isolated from Bixa orellana L., sensitizes human melanoma cells to dacarbazine-induced apoptosis through ROS-mediated cytotoxicity. Food and Chemical Toxicology 125, 549–561. https://doi.org/10.1016/j.fct.2019.02.013
de Oliveira-Júnior, R.G., Alves Ferraz, C.A., de Oliveira, A.P., da Cruz Araújo, E.C., Prunier, G., Beaugeard, L., Groult, H., Picot, L., de Alencar Filho, E.B., El Aouad, N., Rolim, L.A., Almeida, J.R.G. da S., 2022. Bis-nor-diterpene from Cnidoscolus quercifolius (Euphorbiaceae) induces tubulin depolymerization-mediated apoptosis in BRAF-mutated melanoma cells. Chem Biol Interact 355, 1–11. https://doi.org/10.1016/j.cbi.2022.109849
Diaz-Muñoz, G., Miranda, I.L., Sartori, S.K., de Rezende, D.C., Diaz, M.A.N., 2018. Anthraquinones: An Overview, in: Studies in Natural Products Chemistry. pp. 313–338. https://doi.org/10.1016/B978-0-444-64056-7.00011-8
Do Vale, A.E., David, J.M., Dos Santos, E.O., David, J.P., E Silva, L.C.R.C., Bahia, M. V., Brandão, H.N., 2012. An unusual caffeic acid derived bicyclic [2.2.2] octane lignan and other constituents from Cordia rufescens. Phytochemistry 76, 158–161. https://doi.org/10.1016/j.phytochem.2011.09.019
Freitas, H.P.S., Maia, A.I. V., Silveira, E.R., Marinho Filho, J.D.B., Moraes, M.O., Pessoa, C., Costa Lotufo, L. V., Pessoa, O.D.L., 2012. Cytotoxic cordiaquinones from the roots of Cordia polycephala. J Braz Chem Soc 23, 1558–1562. https://doi.org/10.1590/S0103-50532012005000019
Grange, F., 2005. Epidemiology of cutaneous melanoma: Descriptive data in France and Europe. Ann Dermatol Venereol 132, 975–982. https://doi.org/10.1016/S0151-9638(05)79560-0

Haluska, F.G., Tsao, H., Wu, H., Haluska, F.S., Lazar, A., Goel, V., 2006. Genetic alterations in signaling pathways in melanoma. Clinical Cancer Research 12, 2301–2307. https://doi.org/10.1158/1078-0432.CCR-05-2518

Han, Y.-S., Van der Heijden, R., Verpoorte, R., 2001. Biosynthesis of anthraquinones in cell cultures of the Rubiaceae. Plant Cell Tissue Organ Cult 67, 201–220. https://doi.org/10.1023/A:1012758922713

Ji, X.S., Dai, D.C., Wang, Y.T., Cui, J.Y., Li, H.X., Song, X.M., Yi, J.L., Zhou, X.M., 2022. Two new anthraquinone derivatives from Saprosma crassipes H. S. Lo. Nat Prod Res 1–6. https://doi.org/10.1080/14786419.2022.2106483

Júnior, R.G. de O., Ferraz, C.A.A., Silva, M.G. e, Lavor, É.M. de, Rolim, L.A., Lima, J.T. de, Fleury, A., Picot, L., Quintans, J. de S.S., Júnior, L.J.Q., Almeida, J.R.G. da S., 2017. Flavonoids: Promising Natural Products for Treatment of Skin Cancer (Melanoma), in: Natural Products and Cancer Drug Discovery. pp. 161–210. https://doi.org/10.5772/67573

Knight, D.A., Ngiow, S.F., Li, M., Parmenter, T., Mok, S., Cass, A., Haynes, N.M., Kinross, K., Yagita, H., Koya, R.C., Graeber, T.G., Ribas, A., McArthur, G.A., Smyth, M.J., 2015. Host immunity contributes to the anti-melanoma activity of BRAF inhibitors. Journal of Clinical Investigation 126, 1371–1381. https://doi.org/10.1172/jci84828

Locatelli, C., Branco, F., Beatriz, T., 2013. Current Therapies and New Pharmacologic Targets for Metastatic Melanoma, in: Recent Advances in the Biology, Therapy and Management of Melanoma. pp. 1–15. https://doi.org/10.5772/55192

Malik, M.S., Alsantali, R.I., Jassas, R.S., Alsimaree, A.A., Syed, R., Alsharif, M.A., Kalpana, K., Morad, M., Althagafi, I.I., Ahmed, S.A., 2021. Journey of anthraquinones as anticancer agents – a systematic review of recent literature. RSC Adv 11, 35806–35827. https://doi.org/10.1039/D1RA05686G

Manola, J., Atkins, M., Ibrahim, J., Kirkwood, J., 2000. Prognostic factors in metastatic melanoma: A pooled analysis of Eastern Cooperative Oncology Group trials. Journal of Clinical Oncology 18, 3782–3793. https://doi.org/10.1200/JCO.2000.18.22.3782

Marinho-Filho, J.D.B., Bezerra, D.P., Araújo, A.J., Montenegro, R.C., Pessoa, C., Diniz, J.C., Viana, F.A., Pessoa, O.D.L., Silveira, E.R., de Moraes, M.O., Costa-Lotufo, L. V., 2010. Oxidative stress induction by (+)-cordiaquinone J triggers both mitochondria-dependent apoptosis and necrosis in leukemia cells. Chem Biol Interact 183, 369–379. https://doi.org/10.1016/j.cbi.2009.11.030

Matias, E.F.F., Alves, E.F., Silva, M.K. do N., Carvalho, V.R. de A., Coutinh, H.D.M., da Costa, J.G.M., 2015. The genus Cordia: Botanists, ethno, chemical and pharmacological aspects. Revista Brasileira de Farmacognosia 25, 542–552. https://doi.org/10.1016/j.bjp.2015.05.012

Mckee, C.S., Hill, D.S., Redfern, C.P.F., Armstrong, J.L., Lovat, P.E., 2013. Oncogenic BRAF signalling increases Mcl-1 expression in cutaneous metastatic melanoma. Exp Dermatol 22, 767–769. https://doi.org/10.1111/exd.12254

Menzies, A.M., Long, G. V., 2013. Recent advances in melanoma systemic therapy. BRAF inhibitors, CTLA4 antibodies and beyond. Eur J Cancer 49, 3229–3241. https://doi.org/10.1016/j.ejca.2013.06.027

Miller, J.S., Gottschling, M., 2007. Generic classification in the Cordiaceae (Boraginales): Resurrection of the genus Varronia P. Br. Taxon 56, 163–169.

Mund, N.K., Čellárová, E., 2023. Recent advances in the identification of biosynthetic genes and gene clusters of the polyketide-derived pathways for anthraquinone biosynthesis and biotechnological applications. Biotechnol Adv 63, 1–21. https://doi.org/10.1016/j.biotechadv.2023.108104

Nardin, A., Wong, W.C., Tow, C., Molina, T.J., Tissier, F., Audebourg, A., Garcette, M., Caignard, A., Avril, M.F., Abastado, J.P., Prévost-Blondel, A., 2011. Dacarbazine promotes stromal remodeling and lymphocyte infiltration in cutaneous melanoma lesions. Journal of Investigative Dermatology 131, 1896–1905. https://doi.org/10.1038/jid.2011.128

Palmieri, G., Ombra, M.N., Colombino, M., Casula, M., Sini, M.C., Manca, A., Paliogiannis, P., Ascierto, P.A., Cossu, A., 2015. Multiple molecular pathways in melanomagenesis: Characterization of therapeutic targets. Front Oncol 5, 1–16. https://doi.org/10.3389/fonc.2015.00183

Prickett, T.D., Crystal, J.S., Cohen, C.J., Pasetto, A., Parkhurst, M.R., Gartner, J.J., Yao, X., Wang, R., Gros, A., Li, Y.F., El-Gamil, M., Trebska-McGowan, K., Rosenberg, S.A., Robbins, P.F., 2016. Durable complete response from metastatic melanoma after transfer of autologous T cells recognizing 10 mutated tumor antigens. Cancer Immunol Res 4, 669–678. https://doi.org/10.1158/2326-6066.CIR-15-0215

Procházková, E., Kucherak, O., Stodůlková, E., Tošner, Z., Císařová, I., Flieger, M., Kolařík, M., Baszczyňski, O., 2021. NMR Structure Elucidation of Naphthoquinones from Quambalaria cyanescens. J Nat Prod 84, 46–55. https://doi.org/10.1021/acs.jnatprod.0c00930

Valli, M., Dos Santos, R.N., Figueira, L.D., Nakajima, C.H., Castro-Gamboa, I., Andricopulo, A.D., Bolzani, V.S., 2013. Development of a natural products database from the biodiversity of Brazil. J Nat Prod 76, 439–444. https://doi.org/10.1021/np3006875

Van Goietsenoven, G., Hutton, J., Becker, J.P., Lallemand, B., Robert, F., Lefranc, F., Pirker, C., Vandenbussche, G., Van Antwerpen, P., Evidente, A., Berger, W., Prévost, M., Pelletier, J., Kiss, R., Kinzy, T.G., Kornienko, A., Mathieu, V., 2010. Targeting of eEF1A with Amaryllidaceae isocarbostyrils as a strategy to combat melanomas. FASEB Journal 24, 4575–4584. https://doi.org/10.1096/fj.10-162263

Vieira, D.D., Melo, J.I.M. de, Conceição, A. de S., 2015. Boraginales Juss. ex Bercht. & J.Presl in the Ecoregion Raso da Catarina, Bahia, Brazil. Biota Neotrop 15, 1–17. https://doi.org/10.1590/1676-0611-BN-2014-0201

Watanabe, M.T.C., Hiura, A.L., Nogueira, M.G.C., 2017. Flora das cangas da Serra dos Carajás, Pará, Brasil: Cordiaceae. Rodriguesia 68, 955–960. https://doi.org/10.1590/2175-7860201768330

Watroly, M.N., Sekar, M., Fuloria, S., Gan, S.H., Jeyabalan, S., Wu, Y.S., Subramaniyan, V., Sathasivam, K. V, Ravi, S., Mat Rani, N.N.I., Lum, P.T., Vaijanathappa, J., Meenakshi, D.U., Mani, S., Fuloria, N.K., 2021. Chemistry, Biosynthesis, Physicochemical and Biological Properties of Rubiadin: A Promising Natural Anthraquinone for New Drug Discovery and Development. Drug Des Devel Ther Volume 15, 4527–4549. https://doi.org/10.2147/DDDT.S338548

Wisetsai, A., Lekphrom, R., Schevenels, F.T., 2021. New anthracene and anthraquinone metabolites from Prismatomeris filamentosa and their antibacterial activities. Nat Prod Res 35, 1582–1589. https://doi.org/10.1080/14786419.2019.1627352

Zhang, R., Miao, Y., Chen, L., Yi, S., Tan, N., 2022. De Novo Transcriptome Analysis Reveals Putative Genes Involved in Anthraquinone Biosynthesis in Rubia yunnanensis. Genes (Basel) 13, 521–535. https://doi.org/10.3390/genes13030521